Numerical Investigation on Reservoir Heat Production Capacity of a Downhole Heat Exchanger Geothermal System

Yu Shi [1], Xianzhi Song [1,*], Gensheng Li [1], Zhonghou Shen [1], Jinxia Liu [2], Ruixia Li [2], Yiqun Zhang [1], Ruiyue Yang [1], Zehao Lyu [1]

[1] State Key Laboratory of Petroleum Resources and Prospecting, China University of Petroleum, Beijing, Beijing 102249, China
[2] Sinopec Star Petroleum Co. Ltd, Beijing 100083, China

Keywords

geothermal energy; downhole heat exchanger; reservoir properties; natural convection; heat production capacity

ABSTRACT

Reservoir properties have significant impacts on reservoir heat production capacity of a Downhole heat exchanger (DHE) geothermal system. However, few researches are conducted to study this problem. In this paper, an unsteady-state flow and heat transfer model by considering natural convection for DHE system is presented. Subsequently, temperature and velocity fields are analyzed. Influences of key parameters, such as porosity, permeability and rock thermal conductivity on heat production capacity are studied. Simulation results depict that reservoir heat production capacity decreases with the increase of porosity, while it does not reveal obvious trends because of a variation in permeability. As rock thermal conductivity rises, reservoir heat production capacity is improved. If only natural convection exists in reservoir, DHE system could be more suitable for the geothermal field with smaller porosity. Key findings of this work can be used to optimize the geothermal reservoir for DHE.

1. Introduction

With the increasing concern on the environmental pollution due to the use of fossil fuels, the development of clean and renewable resources has attracted global attentions (Panwar et al. 2011; Moomaw et al. 2011; I.P.O.C. Change 2014). As one of promising and clean renewable resource, geothermal energy merits many advantages, such as abundance, environmental friendly and easy exploitation. As a result, we should accelerate the development and utilization of geothermal energy to alleviate energy demand and air pollution.

Extracting groundwater from the geothermal reservoir is the most efficient method to develop geothermal energy. However, if a large amount of geothermal fluid is exploited, the subsurface

water table will decline, which will cause land subsidence and other issues (Kaya et al.2011; Valgar-đur 1997). Therefore, the geothermal fluid should be re-injected into the reservoir to maintain the subsurface water table. At present, the re-injection technology of groundwater in limestone and other karst reservoirs is relatively mature. However, most of the geothermal resources are stored in sandstone reservoirs. As a result, the re-injection of geothermal fluid is quite difficult (Ungemach 2003; Seibt 2003).

In order to ensure the sustainable development and utilization of geothermal resources, DHE geothermal system was proposed several decades before, which absorbs heat only, without extracting any groundwater from the underground aquifer (Lund 2003). The DHE geothermal system has been widely used for space heating in residential and commercial buildings (Lund 1999; Hepbasli 2003; Burnell and Kissling 2005; White 2006). The DHE system consists of a series of tubes or a single U-tube. The DHE is located in a single wellbore, which is filled with geothermal fluid. The working fluid is circulated inside the DHE and then extracts heat from the surrounding geothermal fluid. Thus, the DHE system has a complicated heat transfer process, which includes natural convection of geothermal fluid induced by heat extraction of DHE, heat conduction of reservoir rock, and forced convection if the geothermal fluid flows naturally. The schematic diagram of heat extraction process for DHE geothermal system is shown in **Figure 1**.

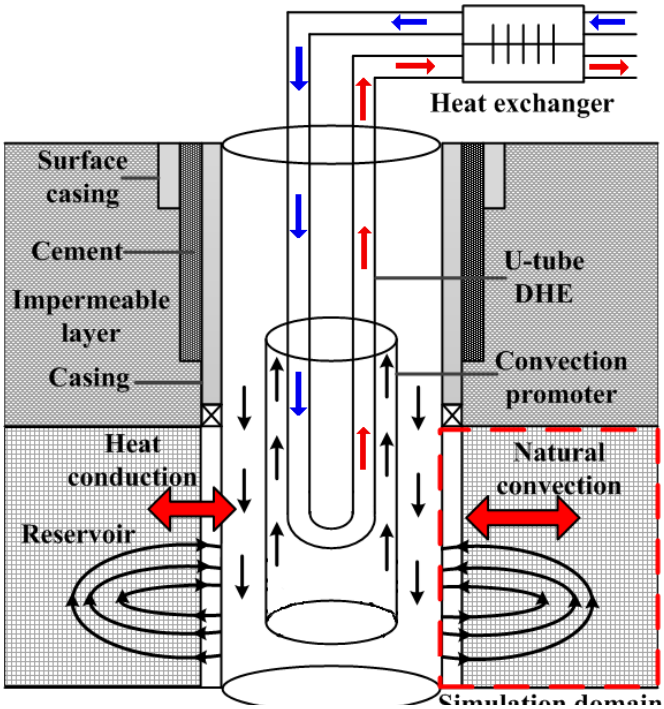

Figure 1: Schematic diagram of DHE geothermal system with a convection promoter

In the 1970s, researchers began to carry out a series of studies on the method of enhancing heat exchange as well as the fluid flow and heat transfer model for DHE system (Allis and James 1980; Carotenuto and Casarosa 2000; Tago et al. 2006; Gustafsson et al. 2010; Steins et al. 2012; Carotenuto et al. 1999; Carotenuto et al. 1997; Carotenuto et al. 2012; Carotenuto et al. 2001; Dai et al. 2011; Lyu et al. 2017). For example, Allis and James (1980) found that a convection promoter tube installed in a borehole could improve the natural convection in the wellbore, and then enhance the heat extraction performance. The installation position and size of the

convection promoter had a significant influence on the DHE performance. Subsequently, Carotenuto and Casarosa (2000) proposed a lumped parameter model to describe the characteristics of fluid flow and heat transfer in wellbore and reservoir matrix in DHE system, and validated the reliability of this model by experiments. Tago et al. (2006) established a fluid flow and heat transfer model of a U-tube DHE with rectangular cross-section, and investigated the influences of working fluid flow rate and DHE materials on the output thermal power of the system. Gustafsson et al. (2010) established a 3D steady-state numerical model for a U-tube DHE, and analyzed the characteristics of temperature and velocity fields for the natural convection in the wellbore. Steins et al. (2012) pointed out that airlifting technique in the DHE systems could enhance geothermal fluid movement and improve the performance of DHE, which obtained a 125% increase in output heat. Carotenuto et al. (2012) utilized a single domain numerical approach to establish a fluid flow and heat transfer model for DHE geothermal system, and optimized the position of the tube casing slotted section to obtain the best heat extraction performance. Lyu et al. (2017) used computational fluid dynamics (CFD) software to study the influences of working fluid flow rate, DHE length and inlet temperature on the thermal power of a U-tube DHE.

Previous researches have made significant contributions to the understanding of the thermal process in DHE geothermal system, and the optimization of the heat transfer performance. However, to the best of our knowledge, few investigations are conducted to analyze the influences of reservoir properties on the reservoir heat production capacity of DHE system. In addition, it is necessary to study the impact of reservoir properties on the maximum heat production capacity of reservoir (Allis and James 1989) and analyze the adaptation of DHE geothermal system. In this paper, an unsteady-state fluid flow and heat transfer model by considering the natural convection is established. Then, based on the geothermal reservoir properties in Bazhou, Hebei, China, the velocity and temperature fields are analyzed comprehensively. The influences of key factors, including temperature difference, porosity, permeability and heat conductivity coefficient of rock, on reservoir heat production capacity are studied. The simulation results in this paper can be used to optimize the geothermal reservoir for DHE system.

2. Numerical model description

2.1 Physical model

The natural convection and heat conduction are the main heat transfer forms for DHE geothermal system. The bottom hole of DHE system is filled with geothermal fluid, from which the working fluid circulated in DHE extracts heat. During this thermal process, the geothermal fluid in the wellbore is cooled down, which results in the density difference between the fluid in the wellbore and geothermal reservoir. Then, buoyancy effect and natural convection are induced. As a result, the cooled geothermal fluid flows out of the borehole, and the hot fluid in the reservoir flows into the borehole. In addition, in order to promote the heat extraction performance of the geothermal system, a convection promoter made of thermal insulation material is often installed at the bottom of the well. The top and bottom of the promoter pipe are open-ended. Because of heat extraction process of DHE, density difference is generated between the inside and outside of the promoter, which enhances the natural convection intensity. Moreover, under the temperature difference between working fluid in DHE and surrounding ground, heat is transferred from

reservoir to wellbore through heat conduction. The heat transfer principles of DHE system is shown in **Figure 1**. Wellbore-wall is set as the computational boundary in this model. The region marked by the red dotted lines is the simulation domain. In the following section, we will present the influences of reservoir properties on the reservoir heat production capacity of DHE system.

2.2 Model assumptions

To describe the natural convection, heat conduction and fluid flow in reservoir matrix, an unsteady-state fluid flow and heat transfer model for geothermal reservoir is established. In the model, we assume that the geothermal reservoir rock is homogeneous and isotropic. Its thermal properties are regarded as constants which do not vary with temperature. According to the temperature and pressure conditions of geothermal reservoir (the pressure is in the range of 10 MPa to 20 MPa and the temperature is in the range of 60 ℃ to 120 ℃), ground water does not vaporize, and is considered as liquid state (Thomson 1946). The density and viscosity of water can be expressed as a function of temperature (Holzbecher 1998):

$$\rho=\begin{cases}1000\times\left(1-\dfrac{(T_c-3.98)^2}{503570}\times\dfrac{T_c+283}{T_c+67.26}\right) & 0℃\le T_c\le 20℃\\ 996.9\times\left(1-3.17\times10^{-4}\times(T_c-25)-2.56\times10^{-6}\times(T_c-25)^2\right) & 20℃\le T_c\le 250℃\\ 1758.4+10^{-3}T\left(-4.8434\times10^{-3}+T\left(1.0907\times10^{-5}-T\times9.8467\times10^{-9}\right)\right) & 250℃\le T_c\le 300℃\end{cases} \quad (1)$$

where ρ is the water density, kg/m^3. T_c represents centigrade degree, ℃, and T represents Kelvin degree, K.

$$\mu=\begin{cases}10^{-3}\times\left(1+0.015512\times(T_c-20)\right)^{-1.572} & 0℃\le T_c\le 100℃\\ 0.2414\times10^{\left(\frac{247.8}{T_c+133.15}\right)} & 100℃\le T_c\le 300℃\end{cases} \quad (2)$$

where μ is the water viscosity, Pa·s.

2.3 Fluid flow model in reservoir matrix

In general, fluid flow in porous media is described by Darcy's law or the Brinkman equation (Nield and Bejan 2013; Bars and Worster 2006). Darcy's law is generally used to model fluid flow with low velocity. And Brinkman equation extends Darcy's law to consider the dissipation of kinetic energy caused by viscous shears, which is formulated as follows:

$$\rho\frac{\partial u}{\partial t}+\rho(u\cdot\nabla)\frac{u}{\varphi}=-\nabla(\varphi p)+\mu\nabla^2u-\frac{\varphi\mu}{K}u+F \quad (3)$$

Since the flow velocity in the porous medium driven by buoyancy force is particularly small, the inertia term (the second term at left hand) is neglected, and the Eq. (3) is simplified as follows:

$$\rho\frac{\partial u}{\partial t}=-\nabla(\varphi p)+\mu\nabla^2u-\frac{\varphi\mu}{K}u+F \quad (4)$$

where ρ is the density of geothermal fluid, kg/m^3. u is the percolation velocity, m/s. φ is the porosity of geothermal reservoir. p is the reservoir pressure, Pa. μ is the viscosity of geothermal

fluid, Pa·s. K is the permeability of reservoir, md. F denotes the volume force. In this work, F represents the buoyancy force caused by density difference, which only exists in the z direction.

According to the Boussinesq approximation (Incropera and DeWitt, 2007), it assumes that the variations of density only affect the buoyancy force term (volume force), and the influences on the pressure term and the viscous force term are ignored. The volume force can be expressed as:

$$F_z = -\rho_r \beta (T - T_r) g \tag{5}$$

where the minus sign indicates that the direction of volume force is opposite to the positive direction of z. ρ_r is the reference density of geothermal fluid, which denotes the fluid density under the original reservoir temperature, kg/m^3. β is the coefficient of thermal expansion for water, which is set as 0.0015 K^{-1}. T_r is the reference temperature, which is the original reservoir temperature in the model, K. g is the gravitational acceleration.

2.4 Heat transfer model

Based on the assumption of local thermal equilibrium (Nield and Bejan 2013), heat exchange between the geothermal fluid and reservoir rock can reach the transient equilibrium state. The energy conservation equation is:

$$(\rho c_p)_{eff} \frac{\partial T}{\partial t} + \rho c_{p,f} u \cdot \nabla T - \nabla (\lambda_{eff} \cdot \nabla T) = Q \tag{6}$$

where T is the temperature, K. $c_{p,f}$ is the heat capacity of geothermal fluid, J/(Kg·K). Q is the heat source term. By assuming no any heat sources in the reservoir, Q is set as zero. $(\rho c_p)_{eff}$ and λ_{eff} are the effective volumetric capacity and the effective thermal conductivity, respectively, which are defined by volume averaging model to account for both reservoir rock and geothermal fluid properties. They can be calculated by:

$$(\rho c_p)_{eff} = (1-\varphi) \rho_r c_{p,r} + \varphi \rho_f c_{p,f} \tag{7}$$

$$\lambda_{eff} = (1-\varphi) \lambda_r + \varphi \lambda_f \tag{8}$$

Where φ represents the reservoir porosity. The subscript f denotes the geothermal fluid, and r indicates the reservoir rock.

3. Initial and boundary conditions

3.1 Initial conditions

The research is focused on the Wumishan Formation of Bazhou geothermal reservoir in Hebei Province, China. We assume that there is no fluid flow driven by natural hydraulic gradient in geothermal reservoir, and the initial velocity is set as zero. The thickness of geothermal reservoir is 200 m. The pressure at the top of the reservoir is 19.6 MPa. The pressure gradient is 9.81×10^3 Pa/m. The temperature at the top of the reservoir is 65 ℃. The temperature gradient is 0.03 ℃/m. In addition, the physical properties of geothermal reservoir in the model are listed in Table 1.

Table 1 Physical properties of reservoir rock

Items	Density (Kg/m^3)	Heat conductivity coefficient (W/(m·K))	Heat capacity (J/(Kg·K))	Permeability (md)	Porosity
Rock	2000	3	1000	100	0.35

3.2 Boundary conditions

The boundary conditions of the simulation model is illustrated in **Figure 2**. Since the impermeable layers are located at the top and bottom of the target reservoir, no-flow boundary conditions are applied. In addition, for the thermal boundary conditions, the Dirichlet boundary is exerted at the wellbore-wall and the reservoir boundary. The initial reservoir temperature is utilized at the side boundary and the temperature of wellbore-wall is set as 25 ℃. The adiabatic condition is applied on the top and bottom boundary.

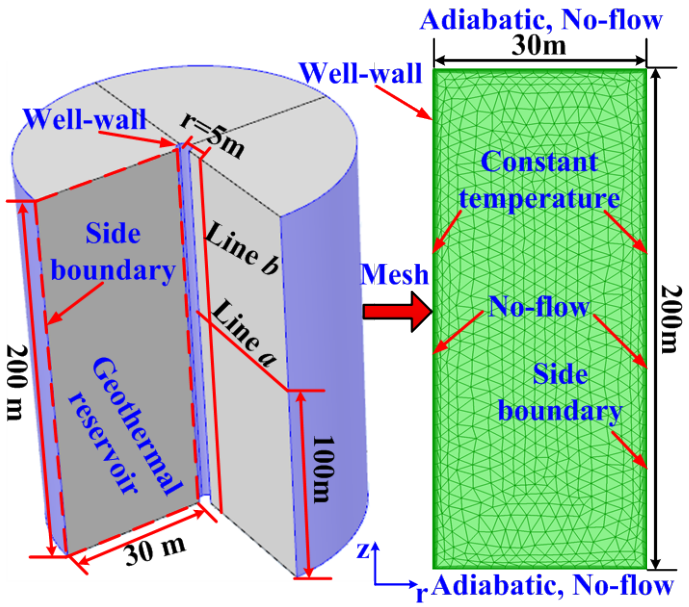

Figure 2: Geometry model, boundary conditions and mesh scheme of the simulation

3.3 Numerical simulation method

In the paper, the finite element solver COMSOL is utilized to solve the partial differential equations of the unsteady-state fluid flow and heat transfer model. Due to the assumption that the geothermal reservoir is homogeneous and isotropic, it is reasonable to neglect the variations of the velocity and temperature along the circumferential direction. Therefore, the model is simplified as a 2D axisymmetric model. Moreover, in the simulation model, the simulation domain has a height of 200 m and a radius of 30 m, which will be proven to be reasonable by the following section. The triangular elements is used in the mesh scheme for the simulation model.

And mesh is refined near the boundaries, as shown in **Figure 2**. For the convenience of the following analysis, Line *b* with a radial distance of 5 m and Line *a* with a vertical distance of 100 m are marked in **Figure 2**. In addition, considering the actual heating duration time during winter in China, the simulation time is set as 4 months, and the time step is set as 1 day.

4. Results and discussion

4.1 Analysis of natural convection velocity field

Figure 3 (a) shows the natural convection velocity contour of reservoir after 120 d for the DHE system. It can be observed that the velocity near the wellbore is the largest, where the fluid flows downwards. And the velocity decreases gradually along the radial direction. At a certain distance (9 m) away from the wellbore, the fluid begin to flow upwards. This is because that the heat extraction process in wellbore causes the decrease of geothermal fluid temperature near the wellbore, subsequently induces the increase of fluid density. The phenomenon is consistent with the regulation of the natural convection. **Figure 3 (b)** displays the isosurface of natural convection velocity. It can be seen that the velocity along the vertical direction almost keeps constant, and the isosurface appears like a cylindrical surface. However, due to boundary effects, the velocity near the boundaries fluctuates greatly, which is consistent with velocity distribution curves along the Line *b* shown in **Figure 4**. **Figure 5** plots the velocity distribution curve along the Line *a*. It can be seen that the seepage velocity decreases with the increase of radial distance, and the seepage velocity increases gradually with time. This is because that the increase of temperature difference results in the increase of the body force. It should be noted that the impact scope of velocity field is only about 9 m after 120 days. The impact scope is much smaller than the radius of simulation domain, which proves that the side boundary has neglected effect on the simulation results, and the simulation domain with a radius of 30 m is reasonable.

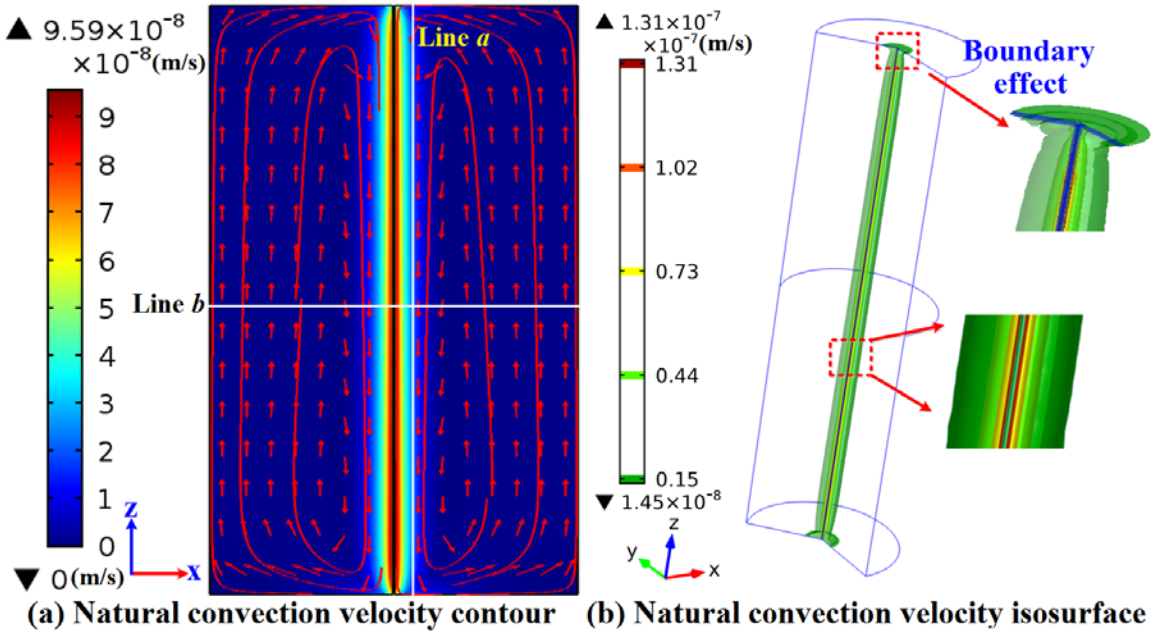

Figure 3: Natural convection velocity field in reservoir matrix after 120 d

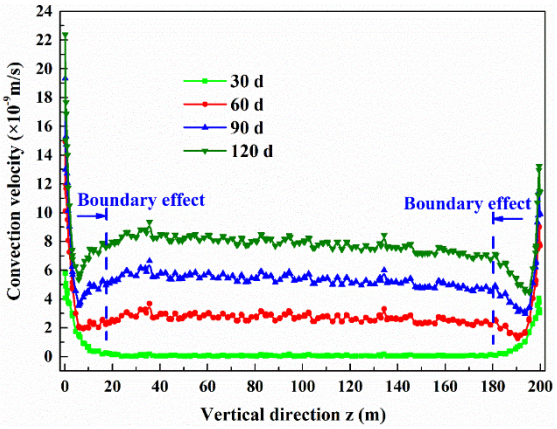

Figure 4: Velocity distribution curve along Line *b* at different time

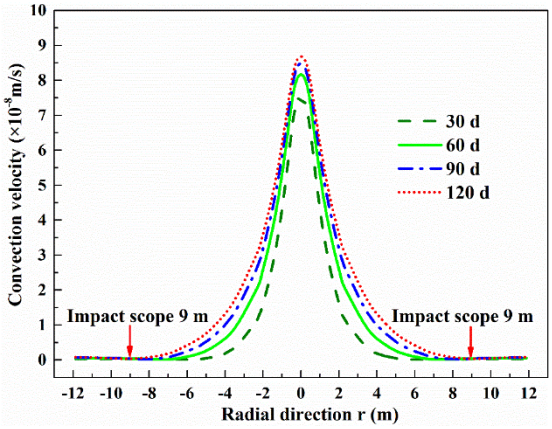

Figure 5: Velocity distribution curve along Line *a* at different time

4.2 Characteristics of temperature field distribution

Figure 6 shows the temperature contour after 120 d, and it can be concluded that the impact scope of temperature field is small during the heating duration (within 4 months). Due to heat extraction, the temperature near the wellbore decreases greatly, forming a funnel-shaped temperature isosurface. **Figure 7** and **Figure 8** plot the temperature distribution curves along Line *b* and Line *a* at different time, respectively. It can be seen from **Figure 7** that the temperature shows a linear distribution along the vertical direction. The temperature declines with time, but the temperature gradient keeps constant. **Figure 8** indicates that the impact scope of temperature field is about 9 m, which is consistent with the impact scope of velocity field. Both of the impact scopes do not reach the side boundary.

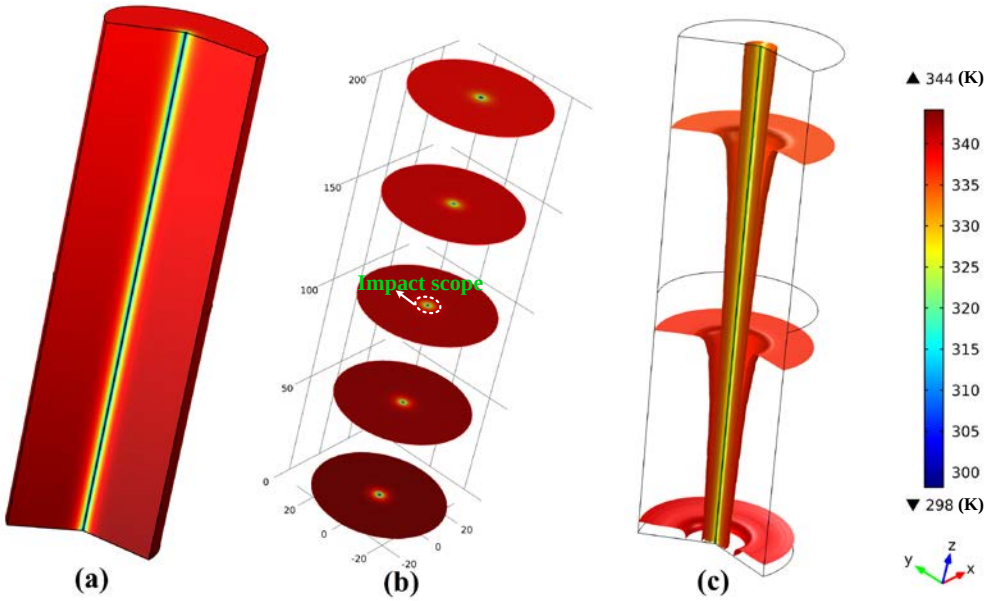

Figure 6: Temperature field after 120 d (a) entire temperature contour; (b) slice temperature contour in the axial direction; (c) temperature isosurface

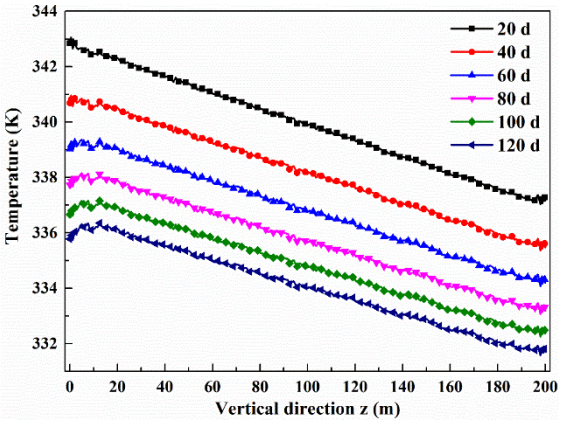

Figure 7: Velocity distribution curve along Line *b* at different time

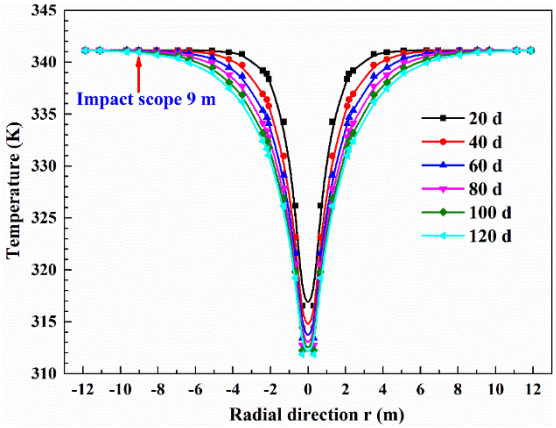

Figure 8: Velocity distribution curve along Line *a* at different time

4.3 The influence of temperature difference

In this paper, the heat production capacity of reservoir represents the thermal power through the wellbore-wall, which is the total heat extracted from surrounding ground. It can be formulated by:

$$P=\int_S qds \tag{9}$$

where P is the thermal power, kW; q denotes the heat flux through wellbore-wall, kW/m^2; S indicates the area of wellbore-wall, m^2.

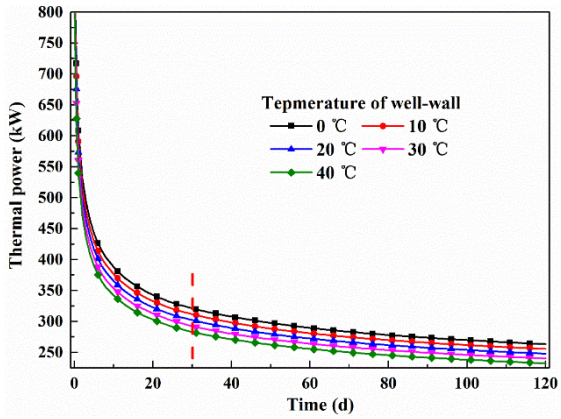

Figure 9: Thermal power under different wellbore-wall temperatures with time

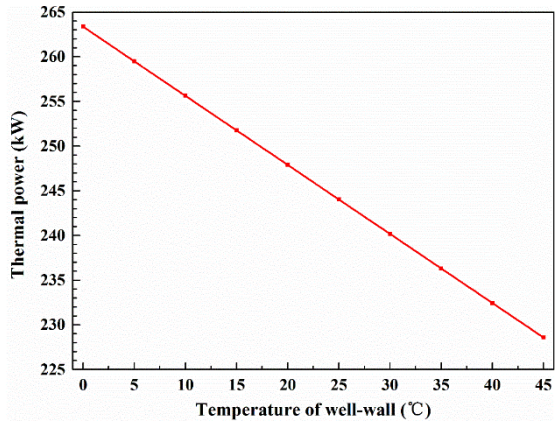

Figure 10: Thermal power with various wellbore-wall temperatures after 120 d

Figure 9 shows the thermal power under different wellbore-wall temperatures along with time. It can be concluded that the thermal power keeps decreasing with time. During the early 30 days, the thermal power decreases rapidly. Subsequently, it remains almost constant. **Figure 10** shows the thermal power under various wellbore-wall temperatures after 120 d, from which we can see that the temperature difference between wellbore-wall and geothermal reservoir has a significant

influence on the thermal power. And the thermal power declines linearly with the decrease of the temperature difference. For example, the thermal power with a wellbore-wall temperature of 45 ℃ is 228.58 kW, which is lower than that with a wellbore-wall temperature of 0 ℃ (263.37 kW). If the thermal power with a wellbore-wall temperature of 0 ℃ is taken as the maximum reservoir heat production capacity, the maximum heat production capacity of Bazhou geothermal field can reach 973.87 kW during the initial production stage. Then it remains about 270 kW after 30 days.

4.4 The influences of reservoir porosity and permeability

Figure 11 shows the thermal power under different reservoir porosity and permeability after 60 d. It can be observed that the porosity has a much more significant influence than the permeability on the thermal power. The thermal power decreases gradually with the increase of porosity, while the thermal power keeps constant as the permeability rises. In order to reveal the reasons leading to the above results, the characteristics of velocity and temperature fields under different reservoir porosity and permeability are analyzed, as shown in **Figure 12** and **Figure 13**. It indicates that the temperature of the reservoir after 60 d with a porosity of 0.4 is higher than that with a porosity of 0.2, and the percolation velocity declines with the increase of porosity. This is because that the thermal diffusivity of geothermal fluid is around 1.55×10^{-7} m^2/s, while the thermal diffusivity of rock is about 1.50×10^{-6} m^2/s. Thus, the thermal diffusivity of rock is about 10 times higher that of geothermal fluid. If the porosity of reservoir increases, the volume ratio of geothermal fluid will increase, which results in the decrease of the overall thermal diffusivity of geothermal reservoir. Therefore, heat flow rate is lower in relatively higher reservoir porosity, retarding the temperature reduction in the reservoir. Subsequently, the buoyancy effect declines and percolation velocity decreases. **Figure 13** indicates that as the permeability increases from 50 md to 100 md, the percolation velocity increases, which resulted from the decrease of flow impedance. However, the temperature in reservoir remains unchanged, which means that the increase of percolation velocity is too small to enhance the heat transfer in reservoir. As a result, it is inferred that if only natural convection exists in geothermal reservoir, the DHE geothermal system could be more suitable for the geothermal field with smaller porosity.

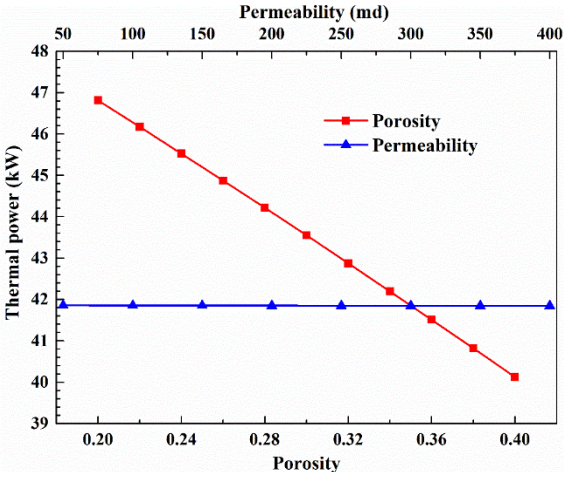

Figure 11: Thermal power under different porosity and permeability after 60 d

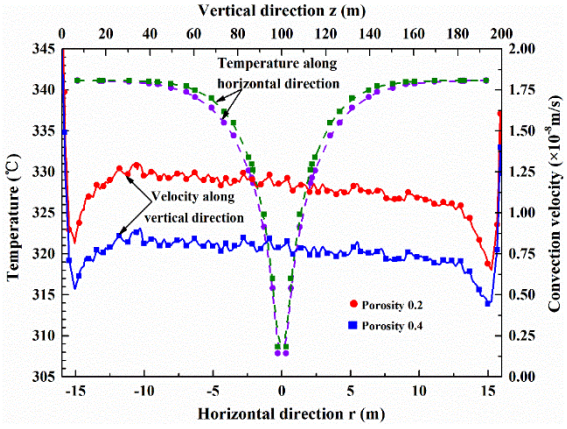

Figure 12: Distributions of convection velocity (along Line *b*) and temperature (along Line *a*) under various porosity after 60 d

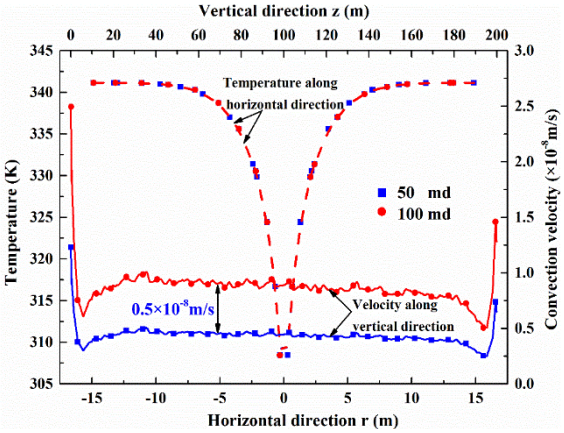

Figure 13: Distributions of convection velocity (along Line *b*) and temperature (along Line *a*) under various permeability after 60 d

4.5 The influences of rock heat conduction coefficient

Figure 14 shows the thermal power under different heat conduction coefficients after 60 d. It can be concluded that the heat conduction coefficient has a major impact on the thermal power. The thermal power increases linearly as the heat conduction coefficient of rock rises. For example, when the heat conduction coefficient of rock rises from 2 W/(m·K) to 4 W/(m·K), the thermal power increases by 69.05%. It means that the heat conduction still plays a leading role in the thermal process of DHE geothermal system.

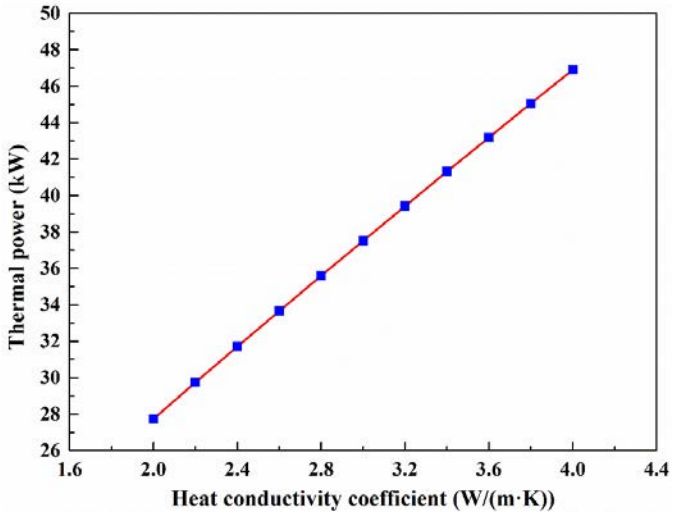

Figure 14: Thermal power under various heat conductivity coefficients after 60 d

5. Conclusion

In this paper, an unsteady-state fluid flow and heat transfer model for the reservoir of DHE geothermal system is established. The finite element solver COMSOL is employed to solve the partial differential equations of the model. The entire velocity and temperature fields are

analyzed comprehensively. The influences of key factors, such as temperature difference, porosity, permeability and thermal conductivity of rock, on heat production capacity of geothermal reservoir are studied. The main conclusions of this study are drawn as follows:

- The velocity near the wellbore is the largest, where the fluid flows downwards. The velocity decreases gradually along the radial direction. At a certain distance (9 m) away from the wellbore, the fluid begin to flow upwards. The temperature shows a linear distribution along the vertical direction and declines with time, but the temperature gradient keeps constant. Besides, both of the impact scopes of temperature field and velocity field are 9 m.
- Reservoir porosity has a much more significant effect than permeability on the reservoir heat production capacity. The thermal power decreases with the increase of porosity. However, when permeability rises, the thermal power remains almost constant. It is inferred that if only natural convection exists in geothermal reservoir, the DHE geothermal system may be more suitable for the geothermal field with smaller porosity.
- The heat conduction coefficient of rock has a great influence on the thermal power. As the heat conduction coefficient of rock increases, the thermal power increases linearly. It indicates that the heat conduction plays a leading role in the thermal process of DHE geothermal system.

ACKNOWLEDGEMENTS

The authors would like to acknowledge the National Key Research and Development Program of China (Grant No. 2016YFE0124600). Besides, support from the Program of Introducing Talents of Discipline to Chinese Universities (111 Plan) (Grant No. B17045) is appreciated.

REFERENCES

Allis R.G. and James R. “Natural-convection promoter for geothermal wells.”, *Geothermal Resources Council Transactions*, United States, 4, (1980), 409-412.

Bars M.L. and Worster M. G. “Interfacial conditions between a pure fluid and a porous medium: implications for binary alloy solidification.” *Journal of Fluid Mechanics*, 550, (2006), 149-173.

Burnell J., and Kissling W. “Rotorua Geothermal Field Management Monitoring Update.” *Environment Bay of Plenty Regional Council*, New Zealand, (2005).

Carotenuto A., Casarosa C., Dell'Isola M., et al. “An aquifer-well thermal and fluid dynamic model for downhole heat exchangers with a natural convection promoter.” *International Journal of Heat & Mass Transfer*, 40, (1997), 4461-4472.

Carotenuto A., Casarosa C. and Martorano L. “The geothermal convector: experimental and numerical results.” *Applied Thermal Engineering*, 19, (1999), 349-374.

Carotenuto A.and Casarosa C. “A lumped parameter model of the operating limits of one-well geothermal plant with down hole heat exchangers.” *International Journal of Heat & Mass Transfer*, 43, (2000), 2931-2948.

Carotenuto A., Casarosa C. and Vanoli L. “Optimizing the position of the tube casing slotted section for geothermal wells with a downhole heat exchanger.” *Geothermics*, 30, (2001), 133-157.

Carotenuto A., Massarotti N. and Mauro A. “A new methodology for numerical simulation of geothermal down-hole heat exchangers.” *Applied Thermal Engineering*, 48, (2012), 225-236.

Dai C., Xie S., Lei H., et al. “A case study of space heating using a downhole heat exchanger in China.” *Geothermal Resources Council Transactions*, 35, (2011), 1077-1080.

Gustafsson A.M., Westerlund L. and Hellström G. “CFD-modelling of natural convection in a groundwater-filled borehole heat exchanger.” *Applied Thermal Engineering*, 30, (2010), 683-691.

Hepbasli A. and Canakci C. “Geothermal district heating applications in Turkey: a case study of Izmir–Balcova.” *Energy Conversion & Management*, 44, (2003), 1285-1301.

Holzbecher E.O. “Modeling Density-Driven Flow in Porous Media.” Springer, Berlin, (1998).

Incropera D. P. and DeWitt D. P. “Fundamentals of Heat and Mass Transfer 6th Ed.” Wiley, (2007).

I.P.O.C. Change. “Climate Change 2014 Synthesis Report.” *Environmental Policy Collection*, 27, (2014), 408.

Kaya E., Zarrouk S.J., and O'Sullivan M.J. “Reinjection in geothermal fields: A review of worldwide experience.” *Renewable and Sustainable Energy Reviews*, 15, (2011), 47-68.

Lund J.W. “Examples of individual downhole heat exchangers systems in Klamath Falls.” *Geo-Heat Center Quarterly Bulletin*, 20, (1999), 20-24.

Lund J.W. “Large downhole heat exchanger in Turkey and Oregon.” *Geo-Heat Center Quarterly Bulletin*, 20, (1999), 17-19.

Lund J.W. “The use of downhole heat exchangers.” *Geothermics*, 32, (2003), 535-543.

Lyu Z., Song X., Li G., et al. “Numerical Analysis of Characteristics of a Single U-tube Downhole Heat Exchanger in the Borehole for Geothermal Wells.” *Energy*, 125, (2017), 186-196.

Moomaw W., Burgherr P., Heath G., et al. “IPCC Special Report on Renewable Energy Sources and Climate Change Mitigation.” *Minerva Cardioangiologica*, 9, (2011), 758-761.

Nield D.A. and Bejan A. “Convection in Porous Media.” Springer, Berlin, 108, (2013), 284-290.

Panwar N.L., Kaushik S.C., and Kothari S. “Role of renewable energy sources in environmental protection: A review.” *Renewable & Sustainable Energy Reviews*, 15, (2011), 1513-1524.

Seibt P., and Kellner T. “Practical experience in the reinjection of cooled thermal waters back into sandstone reservoirs.” *Geothermics*, 32, (2003), 733-741.

Steins C., Bloomer A. and Zarrouk S.J. “Improving the performance of the down-hole heat exchanger at the Alpine Motel, Rotorua, New Zealand.” *Geothermics*, 44, (2012), 1-12.

Tago M., Morita K. and Sugawara M. “Heat extraction characteristics of a single U-tube downhole heat exchanger with square cross section.” *Heat and Mass Transfer*, 42, (2006), 608-616.

Thomson G.W. “he Antoine equation for vapor-pressure data.” *Chemical Reviews*, 38, (1946), 1.

Ungemach P. “Reinjection of cooled geothermal brines into sandstone reservoirs.” *Geothermics*, 32, (2003), 743-761.

Valgar-đur S. “Geothermal reinjection experience.” *Geothermics*, 26, (1997), 99-139.

White B. “An Assessment of Geothermal Direct Heat Use in New Zealand.” *New Zealand Geothermal Association*, (2006).